Progress In Electromagnetics Research, Vol. 142, 107–121, 2013

A HYBRID DETERMINISTIC/METAHEURISTIC SYNTHESIS TECHNIQUE FOR NON-UNIFORMLY SPACED LINEAR PRINTED ANTENNA ARRAYS

Diego Caratelli[1, *], Maria C. Viganó[2], Giovanni Toso[3], Piero Angeletti[3], Alexander Shibelgut[4], and Renato Cicchetti[5]

[1]The Antenna Company Nederland B.V., Grebbeweg 111, 3911 AV, Rhenen, The Netherlands

[2]ViaSat Antenna Systems, EPFL-Quartier de l'Innovation, Bât J, Lausanne 1015, Switzerland

[3]European Space Agency, ESTEC, Keplerlaan 1, 2201 AZ, Noordwijk, The Netherlands

[4]Tomsk State University of Control Systems and Radioelectronics, Lenina Prospect 40, Tomsk 634050, Russia

[5]Sapienza University of Rome, Via Eudossiana 18, Rome 00184, Italy

Abstract—A novel hybrid approach to the synthesis of non-uniformly spaced linear arrays of printed antennas is presented and thoroughly discussed in this paper. In order to account for parasitic mutual coupling between array elements, a dedicated optimization procedure in combination with a multiport network approach is adopted. Selected examples are included in order to assess the effectiveness and versatility of the proposed technique.

1. INTRODUCTION

An advanced hybrid deterministic/metaheuristic approach to the synthesis of non-uniformly spaced linear printed patch antenna arrays [1–3] is presented. A deterministic antenna placement technique, based on the concept of Auxiliary Array Factor (AAF) [4–7], is adopted as a pre-conditioner. In this way, the initial array element locations and excitation distributions useful to mimic a given radiation pattern can be determined analytically while addressing

Received 11 July 2013, Accepted 10 August 2013, Scheduled 21 August 2013

* Corresponding author: Diego Caratelli (d.caratelli@tudelft.nl).

design constraints relevant to the minimum antenna spacing, array aperture, and maximum number of power levels to be operated in the array beam-forming network. The obtained array configuration is afterwards processed within a dedicated Particle Swarm Optimization (PSO) algorithm [8–12] in combination with a multiport network approach [13, 14] for computationally efficient modeling of the parasitic mutual coupling between the antenna elements. Along these lines, an enhancement of the convergence in terms of the number of iterations within the metaheuristic procedure and, consequently, a reduction of the total computational time required to obtain a converged solution of problem can be achieved. This provides an effective design methodology for non-uniformly spaced linear arrays of planar printed antennas in operative scenarios where a significant deviation from ideal antenna operation occurs.

2. DETERMINISTIC ANTENNA PLACEMENT TECHNIQUE

In this section, emphasis is put on the analytical details of the deterministic synthesis procedure used to determine the initial array topology and excitation tapering. The adopted methodology relies on the definition of AAF, which depends on the continuous antenna element density function. Such function is determined by enforcing the equality to a given objective array factor mask in the domain of the Fourier transform with respect to the normalized angular direction parameter. In this way, one obtains an integral equation, involving the element taper, which can be solved analytically or by means of computationally inexpensive numerical methods. Afterwards, the actual antenna positions are evaluated by sampling of the mentioned taper function.

Let us consider a general radiating structure consisting of N_a printed patch antennas deployed over a line as shown in Fig. 1. Where the mutual coupling between the antennas is neglected, the relevant array factor is given by the classical expression [15]:

$$AF(\psi) = \sum_{n=1}^{N_a} \bar{A}_n e^{j[\psi \bar{x}_n/\lambda_0 + \bar{\alpha}_n]}, \tag{1}$$

λ_0 being the wavelength in free space, $\psi = 2\pi \sin\vartheta$ the normalized direction parameter, and $\bar{I}_n = \bar{A}_n e^{j\bar{\alpha}_n}$ the excitation coefficient of the n-th array element located at $x = \bar{x}_n$. As outlined in [4–7], Equation (1) may be regarded as the Riemann's sum approximation

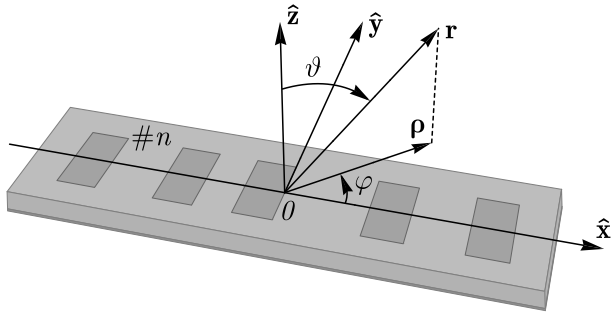

Figure 1. Topology of a general linear aperiodic array of printed patch antennas. The reference system adopted to express the array-related quantities is also shown.

of the AAF defined below:

$$F_A(\psi) = \int_0^{Q_{\max}} \bar{A}(q) e^{j\left[\psi \bar{\xi}(q) + \bar{\alpha}(q)\right]} dq, \tag{2}$$

where $\bar{\xi}(q)$, $\bar{A}(q)$, $\bar{\alpha}(q)$ denote, respectively, the continuous normalized positioning, amplitude and phase distributions which generalize the discrete quantities $\bar{x}_n/\lambda_0$, $\bar{A}_n$, $\bar{\alpha}_n$ appearing in (1). Similarly, q is the continuous version of the index n relevant to the general array element. Upon subdividing the integration domain in (2) in subintervals $[q_{m-1}, q_m]$ with extension $\Delta q = q_m - q_{m-1}$ ($m = 1, 2, \ldots, M$), and performing the piece-wise linearization:

$$\bar{\chi}(q) = \chi_{m-1} + \frac{q - q_{m-1}}{\Delta q} \Delta\chi_m \quad (q_{m-1} \le q \le q_m), \tag{3}$$

with $\chi_m = \bar{\chi}(q_m)$, $\Delta\chi_m = \chi_m - \chi_{m-1}$ for $\chi = \xi, A, \alpha$, the Fourier-transformed AAF can be readily expressed as:

$$\tilde{F}_A(H) = \int_{-\infty}^{+\infty} F_A(\psi) e^{j\psi H} d\psi = \sum_{m=1}^{M} \tilde{F}_{A_m}(H), \tag{4}$$

where each term $\tilde{F}_{A_m}(H)$ is vanishing for $H \notin [-\xi_m, -\xi_{m-1}]$, the relevant magnitude and phase being found to be, after simple mathematical manipulations:

$$\left|\tilde{F}_{A_m}(H)\right| = 2\pi\Delta q \frac{A_{m-1}\left(H + \xi_m\right) + A_m\left(H + \xi_{m-1}\right)}{\Delta\xi_m^2}, \tag{5}$$

$$\arg\left\{\tilde{F}_{A_m}(H)\right\} = \alpha_{m-1} + \frac{\Delta\alpha_m}{\Delta\xi_m}\left(H + \xi_{m-1}\right). \tag{6}$$

The array synthesis is carried out by enforcing $\tilde{F}_A(H) = \tilde{F}_O(H)$, with $\tilde{F}_O(H)$ denoting the Fourier transform of the desired pattern mask $F_O(\psi)$. By virtue of the fact that the distributions $\tilde{F}_{A_m}(H)$ feature non-overlapping support, it is not difficult to figure out that the aforementioned design condition is equivalent, for $H \in [-\xi_m, -\xi_{m-1}]$, to $\tilde{F}_{A_m}(H) = \tilde{F}_O(H)$. In this way, by making use of (5), it follows that:

$$\int_{\xi_{m-1}}^{\xi_m} \left|\tilde{F}_O(-H)\right| dH = \int_{\xi_{m-1}}^{\xi_m} \left|\tilde{F}_{A_m}(-H)\right| dH = \pi\Delta q\left(A_{m-1} + A_m\right). \tag{7}$$

The integral Equation (7) can be solved numerically in combination with a possible constraint on the minimum spacing $d_{\min}$ between the array elements, namely:

$$\Delta\xi_m = \xi_m - \xi_{m-1} \geq \frac{d_{\min}}{\lambda_0}. \tag{8}$$

In this way, one can determine the piecewise linear approximations of the antenna positioning function $\bar{\xi}(q)$ and amplitude tapering $\bar{A}(q)$. Afterwards, the excitation phase distribution is evaluated straightforwardly by implementing the point-matching condition $\arg\{\tilde{F}_{A_m}(H)\} = \arg\{\tilde{F}_O(H)\}$ for $H = -\xi_m$ $(m = 1, 2, \ldots, M)$, which implies:

$$\alpha_m = \arg\left\{\tilde{F}_O(H)\right\}. \tag{9}$$

Finally, the array parameters $\bar{x}_n/\lambda_0$, $\bar{A}_n$, $\bar{\alpha}_n$ in (1) are computed by uniformly sampling of the corresponding continuous functions $\bar{\xi}(q)$, $\bar{A}(q)$, $\bar{\alpha}(q)$, respectively, at the indicial barycenters $q = (n - 1/2)\Delta q$ for $n = 1, 2, \ldots, N_a$, so providing an initial array configuration for the subsequent metaheuristic optimization procedure.

3. MULTIPORT NETWORK MODELING OF THE ARRAY

The wave interaction among radiating elements in a general array environment can influence the performance of the structure dramatically, and therefore has to be properly taken into account during the design process by carrying out a dedicated electromagnetic analysis. To this end, full-wave approaches [16], such as the Finite-Difference Time-Domain (FDTD) technique or the Finite Element

Method (FEM), can be usefully adopted. However, these procedures are typically very time-consuming, especially for large array problems. In this context, the Multiport Network Model (MNM) provides a convenient frame for a computationally efficient and accurate characterization of printed antenna arrays [13]. As a matter of fact, the complexity of this method, as well as the accuracy of the results obtained, lie in between the simplistic transmission line model on one hand, and the numerically based rigorous simulation techniques (like FDTD and FEM) on the other hand.

In the MNM-based characterization of radiating patches (such as the ones shown in Fig. 1), the wave processes occurring in the interior and exterior regions of each element are modeled separately. The interior region underneath the general patch is described by means of a multiport sub-network. On the other hand, the physical phenomena which involve the exterior region, including the radiated, surface wave and fringing field effects, are modeled as external load circuits. The electromagnetic field distribution relevant to the interface between different sub-networks is then matched along the common continuous interface at a discrete number of points corresponding to the ports located all along the periphery of the patch. In doing so, the multiport sub-networks can be conveniently characterized in terms of admittance matrix based representations.

Apart from the usual free-space coupling, the surface waves propagating along the grounded dielectric slab provide an additional coupling mechanism in printed antenna arrays. The effects of the mutual coupling depend on the inter-element spacing, frequency of

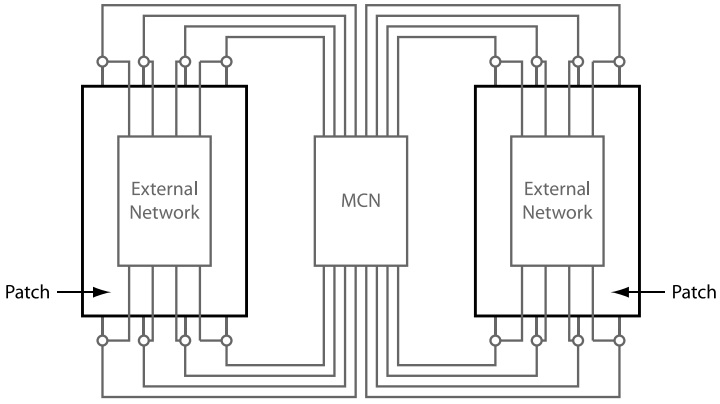

Figure 2. Equivalent multiport network accounting for the mutual coupling between two one-port patch antennas.

operation, as well as the electrical and geometrical characteristics of the dielectric substrate. The multiport network model allows incorporating the effect of mutual coupling among patches in array configuration by defining a Mutual Coupling Network (MCN), as shown in Fig. 2. The ports of the MCN network are connected to the two patches being considered. This may be extended to a larger number of array elements considered in the analysis. As a matter of fact, if a given patch is affected by N adjacent elements, the ports of the relevant MCN will be connected to all these patches. In particular, where thin substrates without dielectric cover layer are adopted (this is actually the assumption in the presented study), the elements of the Y-matrix characterizing MCN networks can be easily obtained from the reaction between the equivalent magnetic current sources at the corresponding sections of the edges of interacting patches, as discussed in [14].

By using the MNM approach, a fast and accurate analysis of the radiation properties of the general printed antenna array sketched in Fig. 1 can be carried out and, in this way, verify whether or not the selected topology and excitation tapering actually result in the desired pattern mask.

4. PSO-BASED ARRAY OPTIMIZATION

Within the proposed synthesis methodology, the array configuration and the relevant parameters $\bar{x}_n$, $\bar{A}_n$, $\bar{\alpha}_n$ $(n = 1, 2, \ldots, N_a)$ are optimized by means of a suitable metaheuristic algorithm in combination with the multiport network modeling detailed in Section 3 in order to compensate for the detrimental effects of parasitic antenna coupling. In this study, attention has been put on the PSO method. The PSO is a robust stochastic evolutionary optimization method based on swarm intelligence [8], and has been successfully applied in the solution of electromagnetic problems regarding antenna design [9–12].

The basic PSO algorithm works by having a swarm of candidate solutions $\mathbf{X}_k = \{\bar{x}_{n,k}, \bar{A}_{n,k}, \bar{\alpha}_{n,k} : n = 1, 2, \ldots, N_a\}$, briefly called particles. The general particle $\mathbf{X}_k$ is moved around in the search-space under the action of a stochastic velocity field $\mathbf{V}_k$, which is function of the best known position $\mathbf{P}_k$ of the particle, as well as of the entire swarm's best known position $\mathbf{G}$. In this way, when improved positions are being discovered, these will then turn to guide the movements of the swarm. The process is iterated till a satisfactory solution is eventually determined. With a simple mathematical formalism, the movement of $\mathbf{X}_k$ at the i-th iteration is updated according to the following equation:

$$\mathbf{X}_k^{(i)} = \mathbf{X}_k^{(i-1)} + \mathbf{V}_k^{(i)}, \tag{10}$$

where:

$$\mathbf{V}_k^{(i)} = \omega\,\mathbf{V}_k^{(i-1)} + a_p\mathbf{R}_p \odot \Delta\mathbf{P}_k^{(i-1)} + a_g\mathbf{R}_g \odot \Delta\mathbf{G}_k^{(i-1)}, \tag{11}$$

with $\Delta\mathbf{P}_k^{(i-1)} = \mathbf{P}_k^{(i-1)} - \mathbf{X}_k^{(i-1)}$ and $\Delta\mathbf{G}_k^{(i-1)} = \mathbf{G}^{(i-1)} - \mathbf{X}_k^{(i-1)}$. In (11) ω denotes the inertia weighting coefficient, and a_p, a_g are suitable acceleration constants, and $\mathbf{R}_p$, $\mathbf{R}_g$ random vectors with uniform distribution over $[0, 1]$. As usual, the symbol $\odot$ indicates the Hadamard product for element-wise multiplication. It is to be noticed that the evolutionary process described by Equations (10)–(11) is performed upon initializing each particle to the solution computed by means of the antenna placement method discussed in Section 1 in such a way as to achieve a faster convergence to the solution. In this respect, it is, also, to be noticed that a subset of the array parameters resulting from the application of the mentioned deterministic synthesis, such as the antenna locations, might be conveniently kept unvaried during the metaheuristic optimization in order to further reduce the computational cost of the procedure.

At each iteration $i > 0$, the goodness of each particle's position is evaluated by a real-valued cost function Υ. This function takes a particle $\mathbf{X}_k^{(i)}$ as argument, and returns the scalar number:

$$\Upsilon\left(\mathbf{X}_k^{(i)}\right) = \sqrt{\int_0^{2\pi} \left|F_O(\psi) - AF\left(\psi, \mathbf{X}_k^{(i)}\right)\right|^2 d\psi}, \tag{12}$$

which represents the objective function value of the given candidate solution expressed in terms of the Euclidean distance between the desired mask $F_O(\psi)$ and the actual array factor $AF(\psi, \mathbf{X}_k^{(i)})$. In particular, $AF(\psi, \mathbf{X}_k^{(i)})$ is computed by using the MNM-based approach as the ratio between the radiation patterns of the array with configuration $\mathbf{X}_k^{(i)}$ and the stand-alone patch antenna element, respectively. In this way, the effects of the parasitic coupling are properly taken into account. The goal is to find a configuration $\mathbf{G}$ in the search-space for which $\Upsilon(\mathbf{G}) \leq \sigma$, with σ being a sufficiently small convergence threshold, according to the flowchart in Fig. 3.

5. NUMERICAL EXAMPLES

The developed methodology has been preliminarily validated by application to the synthesis of a linear array featuring a conventional pencil-beam pattern with side-lobe level $SLL = -20\,\text{dB}$ and angular width $\Theta = 5.5^\circ$ at $-3\,\text{dB}$ level, as shown in Fig. 4. The antenna

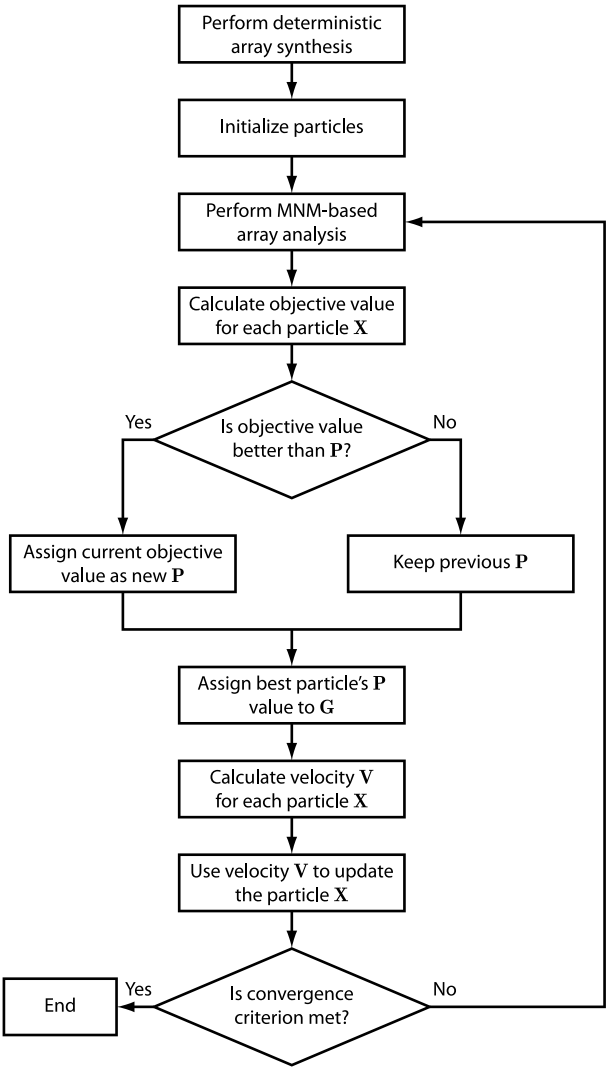

Figure 3. Flowchart of the hybrid deterministic/metaheuristic synthesis technique for non-uniformly spaced printed antenna arrays.

elements consist in square patches with side length $w_p = 21\,\text{mm}$ printed on a dielectric substrate with relative permittivity $\varepsilon_r = 6.15$, loss tangent $\tan\delta = 0.0028$, and thickness $h = 6\,\text{mm}$. The patches are fed by coaxial probes with characteristic impedance $Z_0 = 50\,\Omega$, in such a way as to achieve a resonant frequency $f_0 = c_0/\lambda_0 \simeq 2.5\,\text{GHz}$,

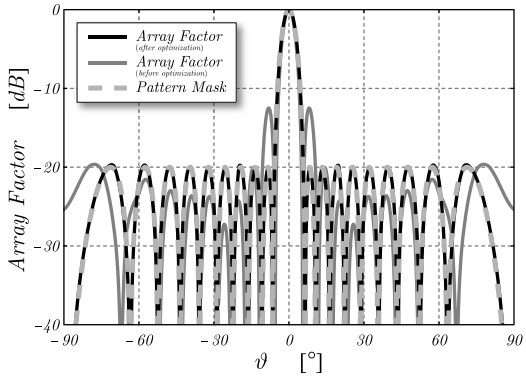

Figure 4. Angular behavior of the synthesized array factor useful to mimic a pencil-beam pattern mask (shown in light-gray dashed line) with side-lobe level $SLL = -20\,\mathrm{dB}$ and angular width $\Theta = 5.5°$. As it can be noticed, the parasitic antenna coupling is responsible for a performance degradation in terms of array side-lobe levels (see dark-gray continuous line) that is compensated by means of the optimization procedure based on PSO and MNM (see black continuous line).

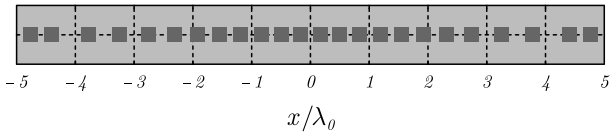

Figure 5. Topology of the non-uniformly spaced patch antenna array featuring the radiation pattern shown in Fig. 4. The overall array aperture is $D_{\max} = 9.725\,\lambda_0$.

c_0 denoting the speed of light in free space. In the considered example, the array aperture has been specified to be $D_{\max} = 9.725\,\lambda_0$.

Subject to the mentioned constraints, the deterministic design methodology has been applied upon selecting the number of antennas as $N_a = 24$. The resulting array topology is sketched in Fig. 5. For sake of clarity, the element positions are listed in Table 1. The minimum inter-element spacing has been found to be $\Delta x_{\min} \simeq 0.341\lambda_0$, whereas the average antenna distance is about $0.425\lambda_0$. The MNM-based analysis of the array configuration obtained using the deterministic antenna placement technique has shown reasonably good characteristics of the radiating structure in terms of return loss, with $|S_{ii}(f_0)| \leq -11.4\,\mathrm{dB}$ for $i = 1, 2, \ldots, N_a$. On the other hand, the maximum parasitic coupling level between the antenna elements has resulted to be far from the value expected in ideal array operation,

Table 1. Antenna locations of the array featuring the radiation pattern shown in Fig. 4.

ELEMENT NUMBER	$\bar{x}_n/\lambda_0$
1	−4.86
2	−4.505
3	−3.853
4	−3.311
5	−2.805
6	−2.37
7	−1.966
8	−1.576
9	−1.215
10	−0.86
11	−0.512
12	−0.171
13	0.17
14	0.511
15	0.859
16	1.214
17	1.575
18	1.965
19	2.369
20	2.805
21	3.311
22	3.853
23	4.505
24	4.86

namely $\max_{i\neq j} |S_{ij}(f_0)| \simeq -8.8\,\mathrm{dB}$. As it can be noticed in Fig. 4, the degradation of the circuital performance of the array results in a significant deviation of the relevant radiation pattern from the desired mask, especially around the first side lobes.

In order to compensate for the effects of the parasitic antenna coupling, the presented PSO-based optimization procedure has been used. In doing so, the needed numerical computations have been performed in double-precision floating-point arithmetic on a workstation equipped with a 2.99 GHz Intel Core Duo processor [17].

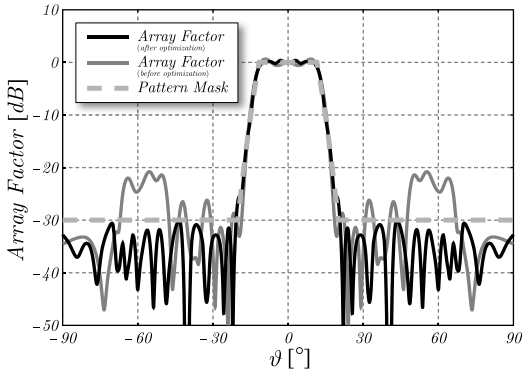

Figure 6. Angular behavior of a flat-top shaped-beam array factor with side-lobe level $SLL = -30\,\mathrm{dB}$ synthesized by means of $N_a = 26$ patch antennas distributed along an aperture having size $D_{\max} = 11.625\,\lambda_0$. The radiation pattern mask is shown in light-gray dashed line.

In this way, by using a two-particle swarm, a converged solution $\mathbf{G}$ of the problem has been obtained after a few iterations, in less than one hour, the final objective function value being $\Upsilon(\mathbf{G}) \simeq 0.05$.

In order to verify the effectiveness and versatility of the proposed design technique, the synthesis of an array featuring a flat-top radiation mask with plateau width $\Phi_p = 23^\circ$ and side-lobe level $SLL = -30\,\mathrm{dB}$ has been, also, carried out (see Fig. 6). As known from the literature, antennas with shaped-beam radiation patterns are widely used in satellite communications [6, 17], as well as synthetic aperture radar (SAR) applications [18, 19], in order to focus the antenna illumination in the region of interest and, in this way, maximize the system performance either in terms of equivalent isotropically radiated power (EIRP) or radiometric accuracy. In the considered example, the array elements have been selected to be square patch radiators printed on a dielectric substrate with relative permittivity $\varepsilon_r = 10.2$, loss tangent $\tan\delta = 0.0035$, and thickness $h = 4.5\,\mathrm{mm}$. The side length ($w_p = 12.6\,\mathrm{mm}$) and feed point of the patches have been optimized in order to achieve proper antenna operation at the working frequency $f_0 = 3\,\mathrm{GHz}$.

By applying the developed synthesis procedure, the aperiodic array topology shown in Fig. 7 has been derived. The structure consists of $N_a = 26$ patch radiators distributed over an aperture with normalized length $D_{\max}/\lambda_0 \simeq 11.625$ at the locations listed in Table 2. As it appears from Fig. 6, the spurious wave interaction between the

array elements is responsible for undesired side radiation lobes and a reduced flatness of the main beam. In this respect, it has been found out that the antenna coupling is such that $\max_{i\neq j}|S_{ij}(f_0)| \simeq -12.3\,\mathrm{dB}$, whereas the input reflection coefficients of the radiating elements satisfy the inequality $|S_{ii}(f_0)| \leq -14.4\,\mathrm{dB}$. To compensate

Table 2. Antenna locations of the array featuring the radiation pattern shown in Fig. 4.

ELEMENT NUMBER	$\bar{x}_n/\lambda_0$
1	−5.8115
2	−5.2535
3	−4.7445
4	−3.7565
5	−3.3765
6	−3.0035
7	−2.6305
8	−2.2555
9	−1.6785
10	−1.3055
11	−0.9325
12	−0.5595
13	−0.1865
14	0.1865
15	0.5595
16	0.9325
17	1.3055
18	1.6785
19	2.2555
20	2.6305
21	3.0035
22	3.3765
23	3.7565
24	4.7445
25	5.2535
26	5.8115

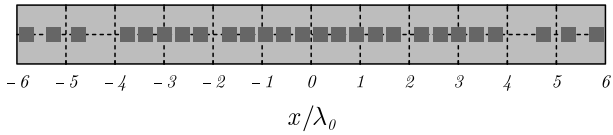

Figure 7. Topology of the non-uniformly spaced patch antenna array useful to mimic the shaped-beam pattern shown in Fig. 6. The minimum inter-element spacing is $\Delta x_{\min} \simeq 0.373\lambda_0$.

for the antenna non-idealities, the PSO-based optimization has been performed using a swarm of four particles, the overall design time being about two hours on the workstation with the aforementioned characteristics. The resulting array architecture nicely meets the pattern requirements with a main-lobe flatness of 0.16 dB.

6. CONCLUSION

A hybrid antenna placement technique for linear aperiodic arrays of planar antennas has been presented. A deterministic method, based on the AAF concept, is used for the preliminary evaluation of the array excitation tapering and element locations which are useful to mimic a desired radiation pattern. The obtained array architecture is afterwards optimized by means of a PSO procedure in combination with the MNM algorithm for computationally fast modeling of spurious mutual coupling processes. In this way, printed antenna array synthesis problems subject to demanding requirements in terms of maximum aperture size and minimum inter-element spacing can be addressed efficiently.

The developed technique has been successfully validated and assessed by application to the synthesis of complex array factor functions arising in wireless communication and radar applications. A generalization of the presented synthesis approach, useful to handle fully two-dimensional sparse array design problems, is currently under development.

ACKNOWLEDGMENT

This research has been partly carried out in the framework of the Sensor Technology Applied in Reconfigurable systems for sustainable Security (STARS) project funded by the Dutch government. For further information, please visit the Web site: http://www.starsproject.nl/.

REFERENCES

1. Kumar, B. P. and G. R. Branner, "Design of unequally spaced arrays for performance improvement," *IEEE Transactions on Antennas and Propagation*, Vol. 47, 511–523, 1999.
2. Donelli, M., S. Caorsi, F. de Natale, M. Pastorino, and A. Massa, "Linear antenna synthesis with a hybrid genetic algorithm," *Progress In Electromagnetics Research*, Vol. 49, 1–22, 2004.
3. Kumar, B. P. and G. R. Branner, "Generalized analytical technique for the synthesis of unequally spaced arrays with linear, planar, cylindrical or spherical geometry," *IEEE Transactions on Antennas and Propagation*, Vol. 53, 621–634, 2005.
4. Caratelli, D. and M. C. Viganó, "A novel deterministic synthesis technique for constrained sparse array design problems," *IEEE Transactions on Antennas and Propagation*, Vol. 59, 4085–4093, 2011.
5. Caratelli, D. and M. C. Viganó, "Analytical synthesis technique for linear uniform-amplitude sparse arrays," *Radio Science*, Vol. 46, 2011, DOI: 10.1029/2010RS004522.
6. Viganó, M. C., G. Toso, P. Angeletti, I. E. Lager, A. Yarovoy, and D. Caratelli, "Sparse antenna array for Earth-coverage satellite applications," *Proc. 4th European Conference on Antennas and Propagation*, 1–4, 2010.
7. Caratelli, D., M. C. Viganó, G. Toso, and P. Angeletti, "Analytical placement technique for sparse arrays," *Proc. 32nd ESA Antenna Workshop*, 2010.
8. Kennedy, J. and R. C. Eberhart, *Swarm Intelligence*, Morgan Kaufmann, San Francisco, 2001.
9. Jin, N. and Y. Rahmat-Samii, "Advances in particle swarm optimization for antenna designs: Real-number, binary, single-objective and multi-objective implementations," *IEEE Transactions on Antennas and Propagation*, Vol. 55, 556–567, 2007.
10. Li, W.-T., X.-W. Shi, and Y.-Q. Hei, "An improved particle swarm optimization algorithm for pattern synthesis of phased arrays," *Progress In Electromagnetics Research*, Vol. 82, 319–332, 2008.
11. Perez Lopez, J. R. and J. Basterrechea, "Hybrid particle swarm-based algorithms and their application to linear array synthesis," *Progress In Electromagnetics Research*, Vol. 90, 63–74, 2009.
12. Liu, D., Q. Feng, and W.-B. Wang, "Discrete optimization problems of linear array synthesis by using real number particle swarm optimization," *Progress In Electromagnetics Research*, Vol. 133, 407–424, 2013.

13. Benalla, A. and K. C. Gupta, "Multiport network model and transmission characteristics of two-port rectangular microstrip antennas," *IEEE Transactions on Antennas and Propagation*, Vol. 36, 1337–1342, 1988.
14. Benalla, A. and K. C. Gupta, "Multiport network approach for modeling the mutual coupling effects in microstrip patch antennas and arrays," *IEEE Transactions on Antennas and Propagation*, Vol. 37, 148–152, 1989.
15. Stutzman, W. L. and G. A. Thiele, *Antenna Theory and Design*, John Wiley & Sons, New York, 1997.
16. Peterson, A. F., S. L. Ray, and R. Mittra, *Computational Methods for Electromagnetics*, Wiley-IEEE Press, New York, 1997.
17. Rao, K. S. and H. J. Moody, "Modelling of shaped beam satellite antenna patterns," *IEEE Transactions on Antennas and Propagation*, Vol. 35, 639–642, 1987.
18. Sharma, S. B., S. Kulshrestha, R. Jyoti, C. Sriharsha, and B. K. Pandey, "Dual-polarized shaped-beam printed antenna for airborne SAR applications," *Microwave and Optical Technology Letters*, Vol. 44, 383–385, 2005.
19. Liu, X., W. Gao, and Y. Deng, "Synthesis technique of array-fed shaped-reflector antenna for DBF-SAR application," *IEEE Antennas and Wireless Propagation Letters*, Vol. 11, 30–33, 2012.